J|A|C|S ARTICLES

Published on Web 03/10/2010

^{14}N Quadrupolar Coupling of Amide Nitrogen and Peptide Secondary Structure As Studied by Solid-State NMR Spectroscopy

Jun Fukazawa,[†,‡] Shin-ichi Kato,[§] Takuo Ozaki,[§] Akira Shoji,[§] and K. Takegoshi*[,†,‡]

Department of Chemistry, Graduate School of Science, Kyoto University, Kitashirakawa Oiwake-cho, Sakyo-ku, Kyoto 606-8502, Japan, CREST, Japan Science and Technology Agency, 4-1-8 Honcho, Kawaguchi, Saitama 332-0012, Japan, and Department of Chemistry and Chemical Biology, Graduate School of Engineering, Gunma University, 1-5-1, Tenjin-cho, Kiryu, Gunma 376-8515, Japan

Received November 24, 2009; E-mail: takeyan@kuchem.kyoto-u.ac.jp

Abstract: To establish a relationship between the secondary structure of a peptide and the quadrupolar coupling of its amide ^{14}N, we examined ^{14}N quadrupolar couplings for eight different polypeptide samples, each of whose secondary structure (α-helix or β-sheet) is known. The ^{14}N quadrupolar coupling is estimated from indirect observation of a ^{14}N overtone resonance under magic-angle spinning. From the observed indirect ^{14}N overtone spectra and calculated ^{14}N quadrupolar couplings for model molecules by using ab initio calculation (Gaussian03), it is shown that the quadrupolar coupling for the α-helix is larger than that for the β-sheet by a few 100 kHz irrespective of the kind of amino acid residues examined (Ala, Val, Leu).

1. Introduction

Amide nitrogens in a main chain of polypeptide/protein play an important role in its structure and dynamics. So far, various studies including spectroscopic investigation using NMR have been done on amide nitrogens. Since the spin quantum number of the abundant isotope of nitrogen, ^{14}N (99.63%), is 1, its NMR signal is influenced by a quadrupolar interaction. Hence, ^{14}N has not been a popular isotope in NMR, and ^{15}N, which is spin-1/2, has been used to study polypeptide/protein structure. So far, the relationship between the secondary structure of a peptide and the isotropic chemical shift or chemical shift tensor components of ^{13}C and ^{15}N in the main chain has been established,[1−3] and a database system (TALOS) for empirical prediction of protein ϕ (C′−N−C$^{\alpha}$−C′) and ψ (N−C$^{\alpha}$−C′−N) backbone torsion angles using isotropic chemical shifts has been developed.[4] Since the ^{14}N quadrupolar interaction reflects the electric field gradient around ^{14}N, it should be sensitive to variation of the local structure. Therefore, it is worthwhile to investigate how the ^{14}N quadrupolar interaction of the amide nitrogen in a peptide is affected by its secondary structure. To avoid effects of dynamic alternation among secondary structures in solution, we applied, in this work, solid-state NMR to study amide ^{14}N nuclei in several polypeptides. For determination of ^{14}N quadrupolar couplings, we adopt ^{14}N overtone NMR[5,6] with an indirect approach, that is, observing the line width of ^{13}C with ^{13}C−^{14}N recoupling by ^{14}N overtone irradiation under magic-angle spinning (MAS).[7,8] Since the ^{14}N overtone transition frequency does not depend on the first-order quadrupolar coupling, the frequency spread of the ^{14}N overtone transition becomes small and efficient irradiation is possible by using the conventional triple resonance circuit. We would like to point out that similar indirect observation of ^{14}N single- and double-quantum spectra proposed by Gan[9] and Cavadini et al.[10] can also be used to examine ^{14}N quadrupolar couplings.

By examining ^{13}C line widths under ^{14}N irradiation for several peptides, each of which the secondary structure (α-helix or β-sheet) is known, we show that the size of the quadrupolar coupling is larger in the α-helix than in the β-sheet. This tendency is further confirmed by ab initio calculation (Gaussian03[11]) applied to elucidate the quadrupolar interaction of the main-chain amide nitrogen in the two model structures ([Ala]$_{18}$[12] and a trimer of [Ala]$_3$) representing an α-helix and β-sheet, respectively. It is also shown that the simulated ^{14}N overtone spectra using the calculated parameters are consistent with the observation.

[†] Kyoto University.
[‡] CREST.
[§] Gumma University.

(1) Mason, J. In *Encyclopedia of NMR*; Grant, D. M., Harris, R. K., Eds.; John Wiley & Sons: Chichester, 1996; Vol. 5, pp 3222−3251.
(2) Ando, I.; Suzuki, S. In *Encyclopedia of NMR*; Grant, D. M., Harris, R. K., Eds.; John Wiley & Sons: Chichester, 1996; Vol. 7, pp 4458−4468.
(3) Shoji, A.; Ando, S.; Kuroki, S.; Ando, I.; Webb, G. A. *Annu. Rep. NMR Spectrosc.* **1993**, *26*, 55–98.
(4) Cornilescu, G.; Delaglio, F.; Bax, A. *J. Biomol. NMR* **1999**, *13*, 289–302.
(5) Tycko, R.; Opella, S. J. *J. Chem. Phys.* **1987**, *86*, 1761–1774.
(6) Stewart, P. L.; Tycko, R.; Opella, S. J. *J. Chem. Soc., Faraday Trans. 1* **1988**, *84*, 3803–3819.
(7) Takegoshi, K.; Yano, T.; Takeda, K.; Terao, T. *J. Am. Chem. Soc.* **2001**, *123*, 10786–10787.
(8) Wi, S.; Frydman, L. *J. Am. Chem. Soc.* **2001**, *123*, 10354–10361.
(9) Gan, Z. *J. Am. Chem. Soc.* **2006**, *128*, 6040–6041.
(10) Cavadini, S.; Lupulescu, A.; Antonijevic, S.; Bodenhausen, G. *J. Am. Chem. Soc.* **2006**, *128*, 7706–7707.
(11) Frisch, M. J.; et al. *Gaussian 03, Revision C.02*; Gaussian, Inc.: Wallingford, CT, 2004.
(12) Shoji, A.; Souma, H.; Ozaki, T.; Kurosu, H.; Ando, I.; Berger, S. *J. Mol. Struct.* **2008**, *889*, 104–111.

 10.1021/ja909931j

Table 1. Samples Used in This Work

sample	structure[a]	major conformation
1	$[Ala^*]_n$	α-helix[b]
2	$[Ala^*,Val]_n$ (40:60)	α-helix
3	$[Leu^*]_n$	α-helix[b]
4	$[Ala]_3$-Ala*-$[Ala]_3$	β-sheet
5	$[Ala^*,Val]_n$ (20:80)	β-sheet
6	$[Leu]_3$-Leu*-$[Leu]_3$	β-sheet
7	$[Val^*]_n$	β-sheet
8	$[Ala,Val^*]_n$ (20:80)	β-sheet

[a] * indicates the (1-^{13}C)-labeled amino acid. For example, $[Ala^*,Val]_n$ (40:60) means the random sequence copolypeptide consisting of Ala* and Val in the ratio of 40 to 60. [b] Containing a small amount of β-sheet.

2. Experimental Section

Eight model peptide samples used in this study were synthesized in our laboratory. The α-helical homopolypeptides containing respective (1-^{13}C)-labeled amino acid residues such as $[Ala^*]_n$, $[Leu^*]_n$, and α-helical $[Ala^*,Val]_n$ (40:60 = composition of 40% of Ala*:60% of Val) were prepared by polymerization of *N*-carboxy-α-amino acid-anhydride (NCA) (where * indicates the (1-^{13}C)-labeled amino acid residue). The β-sheet $[Val^*]_n$, β-sheet $[Ala^*,Val]_n$ (20:80), and β-sheet $[Val^*,Ala]_n$ (80:20) were prepared by polymerization of the mixture of corresponding amino acid NCAs. In addition, we synthesized well-defined heptapeptides adopting a β-sheet form, $[Ala]_3$-Ala*-$[Ala]_3$ and $[Leu]_3$-Leu*-$[Leu]_3$, by solid-phase peptide synthesis using the 9050 PLUS Pepsynthesizer (PerSeptive Biosystems). The synthetic details are shown in our previous paper.[13]

The CO carbon of each peptide is selectively ^{13}C labeled as indicated in Table 1. The secondary structure of each peptide was determined from the ^{13}C chemical shift of the CO carbon.[14] Note that α-helical homopolypeptides, $[Ala^*]_n$ and $[Leu^*]_n$, were predominant, but contained small amounts of a β-sheet.

The NMR experiments were done using a Tecmag APOLLO spectrometer with a MAS probe (Doty Sci. Inc.) for a 5 mm rotor with a single triple-tuned coil oriented along the magic angle. Larmor frequencies for ^{1}H, ^{13}C, and ^{14}N are 299.52, 75.323, and 21.71 MHz, respectively. In this work, the line width dependency of the CO carbon in the peptide bond on the ^{14}N overtone irradiation frequency was measured. The ^{14}N overtone irradiation frequency was varied from 43.310 to 43.409 MHz with a step of 1 kHz. For each ^{14}N overtone frequency, the probe was retuned and a ^{13}C MAS spectrum was recorded under ^{1}H decoupling and ^{14}N overtone irradiation. The radio frequency (rf) strength for ^{1}H decoupling was ca. 80 kHz. The rf strength for ^{14}N overtone irradiation was estimated to be 75 G (46 kHz for ^{14}N overtone resonance) by analyzing the Bloch−Siegert shift[13] of ^{13}C peaks (see below). The MAS speed was 5.5 kHz.

Similar ^{13}C measurements with ^{14}N overtone irradiation for L-alanine and *N*-acetyl-D,L-valine were done by using a homemade spectrometer with a MAS probe (Doty Sci. Inc.) for a 7 mm rotor with a single triple-tuned coil oriented along the magic angle. These amino acid samples were purchased from Aldrich Ltd. and used without purification. Larmor frequencies for ^{1}H, ^{13}C, and ^{14}N are 199.805, 50.246, and 14.44 MHz, respectively. The ^{14}N overtone irradiation frequency was varied from 28.830 to 29.060 MHz with a step of 1 kHz. The rf strength for ^{1}H decoupling was ca. 70 kHz. The rf strength for ^{14}N overtone irradiation was calibrated to be 45 G (28 kHz for ^{14}N overtone resonance) by analyzing the Bloch−Siegert shift of ^{13}C peaks. The MAS speed was 5.35 kHz.

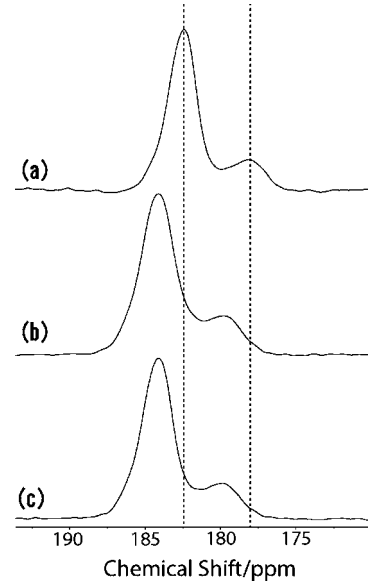

Figure 1. ^{13}C NMR spectra of sample 1: (a) without ^{14}N overtone irradiation, (b) with irradiating at 43.366 MHz, and (c) at 43.350 MHz. Two dotted lines are drawn at 182.4 and 178.0 ppm for eye guidance.

3. Results and Discussion

Figure 1a shows the ^{13}C MAS signal of CO in $[Ala^*]_n$ (sample 1) without ^{14}N overtone irradiation. The peak at the higher frequency (182.4 ppm) is assigned to CO in the α-helix and that at the lower one (178.0 ppm) is the β-sheet. It has been shown that the ^{13}C−^{14}N heteronuclear dipolar interaction leads to an asymmetric doublet signal for the directly bonded ^{13}C spin under MAS when the ^{14}N quadrupolar coupling is larger than a few MHz.[16−19] The intensity ratio for the doublet is 1:2. The smaller signal is ascribed to the ^{13}C signal connected to the $|0\rangle$ spin state of ^{14}N and the larger one to the $|\pm1\rangle$ states. Hence, we expected to observe one 1:2 asymmetric doublet signal for the α-helix CO carbon and another 1:2 doublet for the β-sheet in sample 1. When such a doublet signal can be observed, it is possible to determine the quadrupolar coupling by spectral simulation.[20] Such an asymmetric doublet was, however, not observed for all peptides examined because of the line broadening attributable to the distribution of the local structures of CO in each secondary structure.

Figure 1(b and c) shows the ^{13}C MAS signals of CO in sample 1 under ^{14}N overtone irradiation at 43.366 and 43.350 MHz, respectively. The resonance frequencies of the two peaks move toward higher frequency by ca. 120 Hz under ^{14}N overtone irradiation. This shift is attributed to the Bloch−Siegert shift,[15] and from its size, we estimated the rf irradiation strength for ^{14}N overtone irradiation to be 75 G. Slight but appreciable line broadening is discernible for the α-helix peak (184.0 ppm) under irradiation at 43.366 MHz (Figure 1b), while the broadening occurs at 43.350 MHz for the β-sheet one (179.6 ppm in Figure 1c). The line broadening is ascribed to the recoupling of the

(13) Souma, H.; Shoji, A.; Kurosu, H. *J. Mol. Struct.* **2008**, *889*, 237–243.
(14) Shoji, A.; Ozaki, T.; Saito, H.; Tabeta, R.; Ando, I. *Macromolecules* **1984**, *17*, 1472–1479.
(15) Bloch, F.; Siegert, A. *Phys. Rev.* **1940**, *57*, 522–527.
(16) Hexem, J. G.; Frey, M. H.; Opella, S. J. *J. Am. Chem. Soc.* **1981**, *103*, 224–226.
(17) Opella, S. J.; Hexem, J. G.; Frey, M. H.; Cross, T. A.; Derbyshire, W. *Philos. Trans. R. Soc. London, Ser. A* **1981**, *299*, 665–683.
(18) Zumbulyadis, N.; Henrichs, P. M.; Young, R. H. *J. Chem. Phys.* **1981**, *75*, 1603–1611.
(19) Naito, A.; Ganapathy, S.; McDowell, C. A. *J. Chem. Phys.* **1981**, *74*, 5393–5397.
(20) Naito, A.; Ganapathy, S.; McDowell, C. A. *J. Magn. Reson.* **1982**, *48*, 367–381.

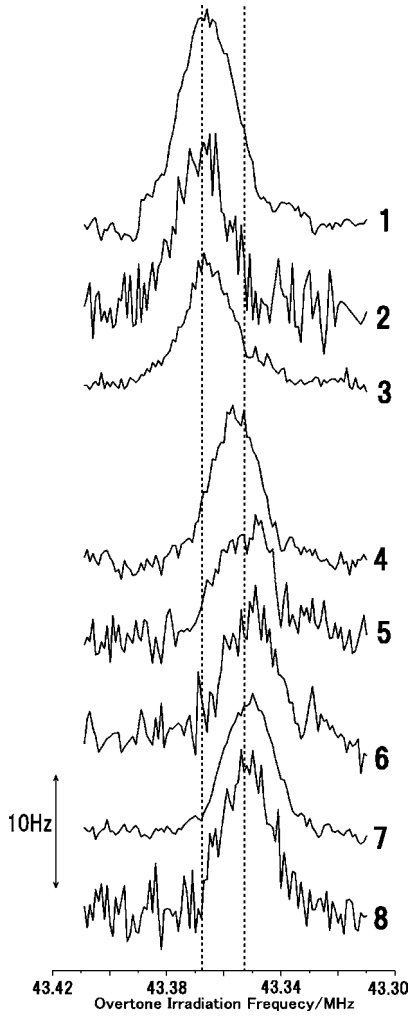

Figure 2. ^{14}N overtone indirect spectra of samples 1−8. The secondary structure of 1−3 is an α-helix and that of 4−8 is a β-sheet. Two dotted lines are drawn at 43.367 and 43.356 MHz for eye guidance.

^{13}C−^{14}N heteronuclear dipolar interaction for the ^{13}C signal connected to the $|\pm1\rangle$ spin states of ^{14}N by ^{14}N overtone irradiation.[7,8] The ^{13}C signal connected to the ^{14}N $|0\rangle$ state is unaffected by the irradiation of first order. The recoupling mechanism has been explained intuitively[7] in terms of modulatory resonance recoupling (MORE)[21] and quantitatively by using the density matrix formalism.[8] To appreciate the recoupling accurately, it is thus necessary to determine the line width of the ^{14}N $|\pm1\rangle$-connected ^{13}C signal in the 1:2 doublet, which is buried in the broad line width for the samples examined in this study. Considering the featureless line shape, we considered that deconvolution is difficult and decided to analyze the overall line width of the merged doublet signal. To obtain the apparent line width for the α-helix and the β-sheet peaks, we fit the observed spectrum to a sum of two Lorenzian line shapes for samples 1 and 3, in which two secondary structures coexist. As the line width thus obtained for the weaker one (the β-sheet in samples 1 and 3) is less accurate, we did not use the β-sheet data obtained for samples 1 and 3 in the following. For the other samples, in which only one ^{13}C signal was observed, we used one Lorenzian for fitting. The line widths obtained are plotted against the ^{14}N overtone irradiation frequency. We shall refer to the plot of the ^{13}C line width versus the ^{14}N overtone irradiation frequency as a ^{14}N overtone indirect spectrum.

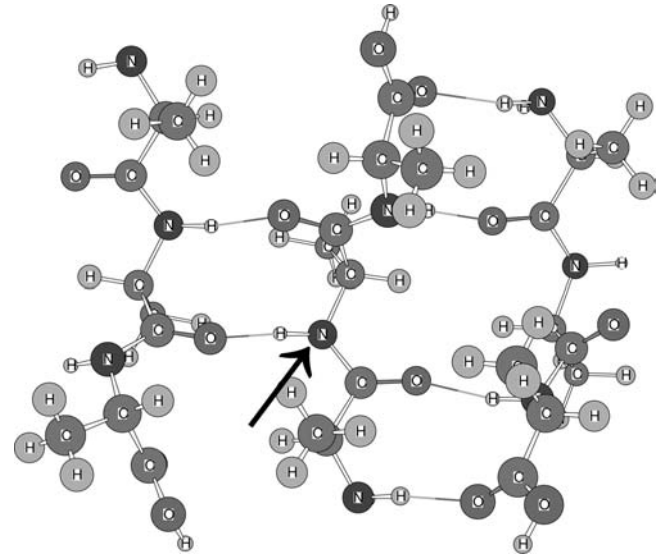

Figure 3. Optimized structure of a trimer of $[Ala]_3$, which is used for the model of an antiparallel β-sheet. Light gray circles denote hydrogen atoms. Hydrogen bonding among the trimer is also plotted. The arrow indicates the nitrogen atom for which quadrupolar parameters are calculated.

In Figure 2, we compare the ^{14}N overtone indirect spectra taken for the CO carbons of samples 1−3, whose secondary structure is an α-helix, and those of samples 4−8, whose secondary structure is an antiparallel β-sheet. For all samples, the line width reaches a maximum at a certain ^{14}N overtone irradiation frequency. Hereafter, we simply refer to the frequency at the maximum line width as the ^{14}N overtone on-resonance frequency. Figure 2 indicates that the ^{14}N overtone on-resonance frequency of the α-helix is ca. 43.367 MHz for samples 1 to 3, which is 10 to 20 kHz higher than those of the β-sheet (43.350−43.356 MHz). As is shown below, this indicates that the absolute value of the quadrupolar coupling constant of the amide ^{14}N in the α-helix is larger than that in the β-sheet. Figure 2 also shows that the ^{14}N quadrupolar coupling constant is less sensitive to the kind of amino acid residue in the peptides. The apparent difference in the ^{14}N overtone on-resonance frequencies for the α-helix and β-sheet can thus be used to differentiate the α-helix ^{13}CO/^{13}C$_\alpha$ carbons in a peptide bonding from those of the β-sheet ones. Such an experiment is under way and will be published elsewhere.

In the following, we estimate ^{14}N quadrupolar coupling constants and asymmetric parameters of the amide ^{14}N spins in the α-helix and β-sheet by using Gaussian03 ab initio calculation. First the secondary-structure models were constructed with a single strand of $(Ala)_{18}$ as α-helix and three strands of $(Ala)_3$ as a β-sheet. The structure of the former has been optimized, and the result is given in ref 12. For the latter, its structure was optimized using HF/STO-3G (Figure 3) as the basis function. The structural data are given in the Supporting Information. The quadrupolar coupling constant and asymmetric parameter were calculated for the central ^{14}N nucleus using the basis set B3LYP/6-311G**.[22,23] For three strands of $(Ala)_3$, we indicated the ^{14}N by an arrow in Figure 3. The calculated results are given

(21) Takegoshi, K.; Takeda, K.; Terao, T. *Chem. Phys. Lett.* **1996**, *260*, 331–335.
(22) Bailey, W. C. *Chem. Phys. Lett.* **1998**, *292*, 71–74.
(23) Tokman, M.; Sundholm, D.; Pyykkö, P.; Olsen, J. *Chem. Phys. Lett.* **1997**, *265*, 60–64.

Table 2. Calculated Quadrupolar Coupling Constants and Asymmetric Parameters for Two Structural Models: α-Helix (a single $(Ala)_{18}$) and β-Sheet (three strands of $(Ala)_3$)

	$(\|e^2Qq\|)/(h)$/MHz	η
α-helix	4.189	0.2683
β-sheet	4.023	0.4399

in Table 2. In accordance with the observed ^{14}N overtone spectra, the absolute value of the calculated ^{14}N quadrupolar coupling constant in the α-helix is larger than that in the β-sheet. We then proceeded to calculate the ^{14}N overtone indirect spectra using these calculated values.

For calculation of the ^{13}C line width under ^{14}N overtone irradiation, we follow a theory developed by Wi and Frydman.[8] In their analysis, the ^{13}C spin echo signals with (S) and without ^{14}N overtone irradiation (S_0) were obtained and the dephasing fractions $(S_0 - S)/S_0$ were plotted against the ^{14}N overtone irradiation frequency. In our experiment, a ^{13}C spectrum under ^{14}N overtone irradiation was observed, and the line width was plotted. Therefore, the $|\pm1\rangle$-connected ^{13}C FID signal $S(\tau)$ is calculated using Wi's equations, while the $|0\rangle$-connected ^{13}C FID signal is assumed to be isotropic and is expressed as 1/3 in the following equation for the total ^{13}C FID written as

$$S_{\mathrm{all}}(\tau) = \frac{1}{3} + \frac{2}{3}\left(\frac{1}{8\pi}\int_0^{2\pi}\int_0^{\pi}\int_0^{2\pi} S(\tau)\mathrm{d}\alpha \sin\beta\, \mathrm{d}\beta\, \mathrm{d}\gamma\right) \quad (1)$$

Effects of MAS on the ^{14}N quadrupolar Hamiltonian (H_{Q}) and ^{13}C−^{14}N dipolar−dipolar Hamiltonian (H_{IS}) are described by adopting the following transformation of the frames for H_{IS},

$$\mathrm{PAS}(D) \xrightarrow{\Omega_3 = \{0^c, \xi, \psi\}} \mathrm{PAS}(Q) \xrightarrow{\Omega_2 = \{\alpha, \beta, \gamma\}} \mathrm{ROTOR} \xrightarrow{\Omega_1 = \{\omega_r t, 54.7^c, 0^c\}} \mathrm{LAB} \quad (2)$$

and for H_{Q},

$$\mathrm{PAS}(Q) \xrightarrow{\Omega_2 = \{\alpha, \beta, \gamma\}} \mathrm{ROTOR} \xrightarrow{\Omega_1 = \{\omega_r t, 54.7^c, 0^c\}} \mathrm{LAB} \quad (3)$$

where the Euler angles Ω_3 describe the orientation of the principal axis system along the internuclear ^{13}C−^{14}N dipole tensor (PAS(D)) from the principal axis system of the quadrupole (PAS(Q)), Ω_2 describes the orientation of the PAS(Q) in the MAS rotation frame (ROTOR), and Ω_1 describes the ROTOR in the laboratory frame (LAB). In following the theory presented by Wi and Frydman[8,25] a number of minor typos were detected, summarized for completion in the Supporting Information.

To examine the legitimacy of the derived equations, we compare the ^{14}N indirect overtone spectra of L-alanine and *N*-acetyl-D,L-valine, whose quadrupolar coupling constants and asymmetric parameters are known (e^2qQ/h = 1.148 MHz and η = 0.276 for L-alanine,[26] and e^2qQ/h = 3.21 MHz and η = 0.31 for *N*-acetyl-D,L-valine[27,28]) with the calculated ones using eq 1. For the integration of the Euler angle set Ω_2, we used the 6044-point set of ZCW3;[29] for Ω_3, we simply set $(\xi, \psi) = (-120, 0)$ and used the N−C distance of 0.142 nm. The $S_{\mathrm{all}}(\tau)$ calculated for a certain ^{14}N overtone irradiation frequency is Fourier transformed, and the resulting ^{13}C line shape is fitted to a single Lorenzian line shape to obtain the line width. Figure 4a shows the observed (dotted line) and the simulated (solid line) indirect ^{14}N overtone spectra of L-alanine, and Figure 4b compares those of *N*-acetyl-D,L-valine. Figure 4 shows that the simulation can reproduce the frequency range for ^{13}C line broadening well, showing that the present experiment is useful for the examination of the size of the quadrupolar interaction. As for the spectral feature, the agreement is not very good. Lineshape dependence on (ξ, ψ) is briefly examined by comparing line shapes calculated for $(\xi, \psi) = (45, 45)$ and $(\xi, \psi) = (-120, 0)$ (Supporting Information), which indicates the line shape does not significantly depend on (ξ, ψ). Since the reproduction of the ^{14}N indirect spectra of these amino acids is not the aim of this work, we did not further examine the line shape.

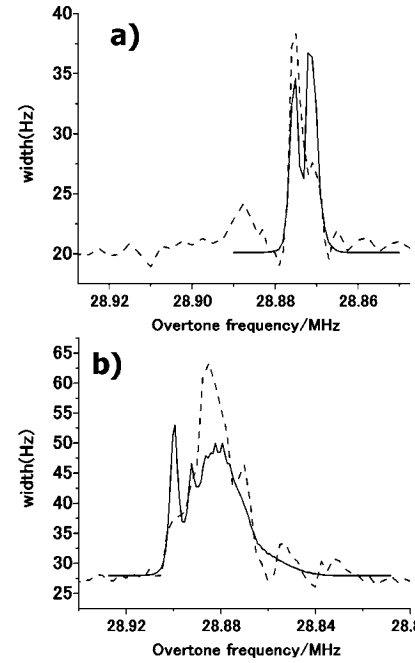

Figure 4. (a) ^{14}N indirect overtone spectra of L-alanine and (b) *N*-acetyl-D,L-valine. The dotted line is the observed one and the black line is the simulated one. In the simulation, we used the C−N bond length of 0.142 nm and Ω_3 was assumed to be $(\xi, \psi) = (-120, 0)$.

Figure 5 compares the two simulated ^{14}N indirect overtone spectra using the calculated-quadrupolar parameters for the α-helix and β-sheet (Table 2) and observed ones. For calculation, we again simply set the angles $(\xi, \psi) = (-120, 0)$ and used the N−C distance of 0.142 nm. It shows that the calculated indirect ^{14}N overtone spectrum of α-helix appears at ca. 10 kHz higher frequency as compared to that calculated for the β-sheet. The direction and the size of this difference are consistent with the observation (Figure 2). Note that the calculated size of the line broadening is much larger than the observed one. This is ascribed to our simplified analysis of the line width; the overall line width of the merged 1:2 doublet signal is less sensitive to the change in one of the doublet peaks. For a sample with better

(24) Naito, A.; Ganapathy, S.; Raghunathan, P.; McDowell, C. A. *J. Chem. Phys.* **1983**, *79*, 4173–4182.
(25) Marinelli, L.; Wi, S.; Frydman, L. *J. Chem. Phys.* **1999**, *110*, 3100–3112.
(26) Takegoshi, K.; Hikichi, K. *Chem. Phys. Lett.* **1993**, *206*, 450–454.
(27) Stark, R. E.; Haberkorn, R. A.; Griffin, R. G. *J. Chem. Phys.* **1978**, *68*, 1996–1997.
(28) Sadiq, G. F.; Greenbaum, S. G.; Bray, P. J. *Org. Magn. Reson.* **1981**, *17*, 191–193.
(29) Edén, M.; Levitt, M. H. *J. Magn. Reson.* **1998**, *132*, 220–239.

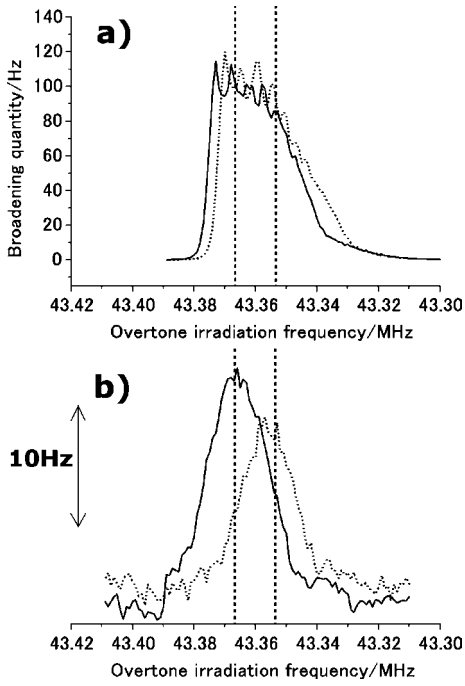

Figure 5. (a) Simulated ^{14}N indirect overtone spectra for α-helix (solid line) and β-sheet (dotted line) using the quadrupolar parameters in Table 2 and (b) observed ^{14}N indirect overtone spectra of sample 1 (solid line) and sample 4 (dotted line).

crystallinity, it is expected that more apparent broadening caused by ^{14}N on-resonance overtone irradiation can be observed.

Lastly, we would like to discuss the molecular reason for the larger quadrupolar coupling constant in the α-helix than in the β-sheet structure. The main reason for the observed difference is most likely related to the difference in hydrogen bonding. Our naive expectation is that a longer N−H bond distance would alleviate the electric field gradient at N, thus leading to a smaller quadrupolar coupling constant. The N−H distances in the calculated α-helix and the β-sheet structures are 0.102 and 0.103 nm, respectively, while the hydrogen-bonding distances (the O to H distance in the CO−HN hydrogen-bonding moiety) in the calculated α-helix and the β-sheet structures are 0.206 and 0.179 nm, respectively, indicating stronger hydrogen bonding in the β-sheet. The difference in the calculated N−H distances is consistent with our expectation; however, the difference is too small and further studies are imperative.

4. Concluding Remarks

It has been shown that the size of the ^{14}N quadrupolar coupling of an amide nitrogen in peptides depends apparently on their secondary structure, and less on the kind of amino acid residue in the peptides, showing the amide ^{14}N quadrupolar interaction is mostly determined by its local structure. The ^{14}N overtone irradiation frequency that results in the largest line broadening for the amide CO carbon differs by ca. 10−15 kHz at 7 T for the α-helix and the β-sheet. Hence it is possible to use this to assign the secondary structure of a residue using the line width of its CO carbon under ^{14}N overtone irradiation. Further with using an echo technique, a selective observation of the CO/C_α carbons belonging to either of the two secondary structures may be realized. These works are in progress and will be published elsewhere.

Acknowledgment. This research was supported by a Grant-in-Aid for the Global COE Program, "International Center for Integrated Research and Advanced Education in Materials Science", from the Ministry of Education, Culture, Sports, Science and Technology of Japan.

Supporting Information Available: Wi's theory (corrected), the influences of structural data on the line shape, and the data of the β-sheet model structure for which the trimer of $[Ala]_3$ is ab initio calculated. This material is available free of charge via the Internet at http://pubs.acs.org.

JA909931J